Author Version of : Marine Chemistry, vol.231; 2021; Article no: 103938

Dry-deposition of inorganic and organic nitrogen aerosols to the Arabian Sea: Sources, transport and biogeochemical significance in surface waters

Poonam Bikkina[1,*], V.V.S.S. Sarma[1], Kimitaka Kawamura[2], Srinivas Bikkina[2]
[1]CSIR-National Institute of Oceanography, Regional Centre,
Visakhapatnam 530017, Andhra Pradesh, India
[2] Chubu Institute for Advanced Studies, Chubu University,
Kasugai-shi, Aichi, 487-8501, Japan
*Corresponding author
Dr. Poonam Bikkina (ptyagi@nio.org)

Abstract

Air-to-sea deposition of water-soluble total nitrogen (WSTN) can influence the primary productivity in the coastal oceans. Here, we assessed the concentrations of aerosol inorganic (WSIN: NH_4^+ + NO_3^-) and WSTN over the Arabian Sea during winter season (SS379:6-24 December 2018). The mean concentrations of NH_4^+ (109±83 nmol m^{-3}) overwhelm that of NO_3^- (32±13 nmol m^{-3}) and water-soluble organic nitrogen (WSON: WSTN-WSIN: 86±81 nmol m^{-3}), and contributing to ~50±31% of WSTN mass. Significant linear relationships of WSON with water-soluble organic carbon and NH_4^+ with non-sea-salt (nss)-K^+ is observed suggesting their common origin from biomass burning and fertilizers. Backward air mass trajectories and satellite-based fire counts further revealed their provenance in the Indo-Gangetic Plain and southern India. The concentration of NO_3^- moderately correlated with nss-Ca^{2+} (dust tracer), indicating heterogeneous reactive uptake on mineral aerosol surface. Despite high concentrations, the deposition fluxes of NH_4^+ (~9.4±7.1 µmol m^{-2} d^{-1}) and WSON (7.4±7.0 µmol m^{-2} d^{-1}) are lower than NO_3^- (27±11 µmol m^{-2} d^{-1}) because of their predominant fine nature (*i.e.*, strong correlation with nss-SO_4^{2-}). We also constrained the total annual atmospheric deposition rates of WSIN (0.94 Tg yr^{-1}) and WSON (0.08 Tg yr^{-1}) to the Arabian Sea during the continental outflow (November-April). The maximum dry-deposition of WSON to the Arabian Sea (0.24 Tg yr^{-1}) is twice that of the riverine supply (0.11 Tg yr^{-1}), highlighting the significance of aeolian sources. By using Redfield Stoichiometry, the WSTN deposition (21-73 µmol m^{-2} d^{-1}) can account for <5.3% of fixed-carbon by a primary production in the Arabian Sea.

Keywords: Water-soluble organic nitrogen, ammonia, marine aerosols, Arabian Sea, continental transport.

Introduction

Atmospheric transport and deposition of reactive nitrogen species, which is one of the major sources of macronutrient to open ocean waters, have a profound influence on biogeochemical cycles of carbon and nitrogen through phytoplankton primary production (Krishnamurthy et al., 2007; Duce et al., 2008; Mahowald et al., 2017). Besides, coastal seas that are located downwind of pollution sources are more vulnerable by the air-sea deposition of particulate nitrogen species, per se reflected through the eutrophication/acidification processes (Doney et al., 2007; Krishnamurthy et al., 2009). For instance, the growing emission of atmospheric anthropogenic nitrogen (*e.g.* biomass burning, forest fires, excessive use fertilizers) in the continental outflows from the Asian regions are shown to influence surface waters of marginal seas (Bikkina et al., 2011; Zhu et al., 2013; Kanakidou et al., 2016).

Atmospheric aerosol nitrogen includes the contribution from both inorganic (NH_4^+ and NO_3^-) and organic nitrogen species (*e.g.* amines; (Facchini et al., 2008; Miyazaki et al., 2010a). Most of the studies on the atmospheric deposition to surface seawater have focused on water-soluble inorganic nitrogen (WSIN) species and, not much is known about the sources of aerosol organic nitrogen in the atmosphere (Jickells et al., 2013). Until recently, rather sparse observations have focused on water soluble organic nitrogen (WSON) levels in the atmosphere (Spokes et al., 2000; Zhang et al., 2002; Cornell et al., 2003). Bronk et al. (2007) suggested that WSON is much more bioavailable than previously thought. Ever since, the WSON component has received considerable attention (Lin et al., 2010; Cape et al., 2011; Cornell, 2014; Miyazaki et al., 2014; Mochizuki et al., 2016) and, in particular, some datasets are now available from the remote and coastal oceans (Nakamura et al., 2005; Lesworth et al., 2010; Miyazaki et al., 2010b; Bikkina et al., 2011; Miyazaki et al., 2011; Qi et al., 2013; Bikkina et al., 2015; Matsumoto et al., 2017). These studies have suggested that WSON could contribute as high as 25-35% of water-soluble total nitrogen (WSTN) in ambient aerosols (Cape et al., 2011; Cornell, 2011; Jickells et al., 2013). Recent modelling studies have projected a 3-4-fold increase in the external nitrogen supply to the surface waters that are downwind of pollution sources in South and Southeast Asia (Jickells et al., 2017).

The Arabian Sea is significantly influenced by the continental outflow from South Asia during the winter season (Bikkina and Sarin, 2013) similar to its eastern counterpart of the northern Indian Ocean, Bay of Bengal. Only a handful of studies have reported the N_{Org} concentrations and dry-deposition fluxes of aerosol-N from the Bay of Bengal (Bikkina et al., 2011; Bikkina et al., 2015). In contrast, rather limited reports are available on the sources and transport patterns of particulate nitrogen species over the Arabian Sea (Sarin et al., 1999; Bikkina and Sarin, 2013). Using

the reported inorganic nitrogen levels in aerosols, Singh et al. (2012) compared the estimated dry-deposition fluxes with the new production supported by N-flux in the surface waters and concluded that aeolian supply is not a significant contributor. Considering the sparse observations on the aerosol inorganic nitrogen (WSIN) data from this marine basin, we attempted here to assess the concentrations of WSIN and WSON over the Arabian Sea. These atmospheric abundances are examined with respect to the origin of air masses, that is, in a way linked to their contribution from geographically varying sources. Furthermore, we compared the atmospheric abundances from the Arabian Sea with those reported over the Bay of Bengal during winter cruise (*i.e.*, when the continental outflow is more severe) to understand relative importance of organic versus inorganic nitrogen over both marine basins of the northern Indian Ocean.

2. Methodology

2.1. Site description, cruise track and meteorology

The Arabian Sea, a western limb of the northern Indian Ocean, is surrounded by the deserts in the Oman, Somalia, Iran, and Thar regions. This marine basin is influenced by the seasonally reversing monsoonal winds, that is, northeasterly in winter and southwesterly in summer (Wiggert et al., 2005). The Arabian Sea is also considered as one of the most productive oceanic basins of the world (Marra and Barber, 2005; Naqvi et al., 2005). Numerous field studies have suggested that the primary productivity in the Arabian Sea is largely governed by the upwelling along the Oman coast during summer and the convective mixing in winter in the northern Arabian Sea (Patra et al., 2007). We collected the aerosol samples onboard FORV Sagar Sampada (SS379), conducted in the offshore waters of the Arabian Sea, started at Kochi on 6 December 2018 and ended at Okha port in Gujarat on 25 December 2018. Figure 1 depicts the cruise track adopted for this study as well as moderate resolution imaging spectroradiometer (MODIS) based Chlorophyll-a data in the Arabian Sea.

The air mass over the Arabian Sea is strongly influenced by the continental pollution sources (*e.g.* biomass burning and fossil-fuel combustion) in winter (November-February) (Bikkina et al., 2011; Kumar et al., 2012; Aswini et al., 2020) and mineral dust particles in summer (March-June) (Tindale and Pease, 1999; Prospero et al., 2002; Kumar et al., 2008). Therefore, the ideal choice of sampling period for assessing the effects of atmospheric deposition of nitrogen to the Arabian Sea is the winter period. It is important to clarify here that, though wet scavenging is considered as a major source of aerosol-N to the seawater, the precipitation events over the Arabian Sea during the continental outflow are rather scarce and episodic. This makes the dry-deposition

estimates serve as the total depositional flux of aerosol-N to the Arabian Sea. A detailed description about prevailing meteorology over the Arabian Sea can be found in Bikkina et al. (2020).

2.2. Aerosol collection and analysis of nitrogenous species

A total of 17 aerosol samples were collected on precombusted (at 450ºC for 6 h) tissue quartz filter (PALLFLEX$^{®TM}$) substrates using a high-volume total suspended particulate matter (TSP) air sampler (flow rate: 1.01 m^3 min^{-1}). The TSP sampler (Envirotech Pvt. Ltd.) was set up on the bridge in front of Ship's navigation room at a height of ~10 m above sea level. We operated the air sampler only when the ship is cruising at a speed of 10 knots per hour and winds from the bow side to avoid any contamination from the ship's exhaust. The filtered air volume varied between 1230 m^3 and 1400 m^3 for most of the TSP samples (except three). After collection, the aerosol filters were wrapped in a precombusted aluminum foil and sealed in airtight Ziploc bags. These filters were subsequently stored at -20 °C until further analysis. The TSP concentration (i.e., normalized for air volume filtered; µg m^{-3}) was ascertained gravimetrically by the difference in weights of aerosol filters before and after sampling. For more details about the aerosol sampling and meteorological parameters during the cruise period, see Bikkina et al. (2020).

Water soluble inorganic species (WSIS) were analyzed using the methodology described in Bikkina et al. (2020) and Boreddy and Kawamura (2015). A 16 mm diameter filter punch of TSP sample was extracted with ultrapure deionized water (specific resistivity >18.2 MΩ-cm) using an ultrasonicator water bath for about 30 min. The extract was filtered through the 0.22 µm disc (PVDF, Millex-GV) to remove the suspended solids and the filtrate was subsequently analyzed for NH_4^+ and NO_3^- on Metrohm Ion Chromatograph (IC 761; (Bikkina et al., 2020)). We eluted cations isocratically (flow rate: 1.0 ml min^{-1}) on METROSEP Cation 1-2 column using a mixture of 5 mM tartaric acid, 1 mM dipicolinic acid and 24 mM boric acid. Likewise, anions were eluted on Shodex IC SI-90 4E column using a mixture of 1.8 mM Na_2CO_3 and 1.7 mM $NaHCO_3$ (flow rate = 1.2 ml min^{-1}). The ion chromatograph was calibrated with the gravimetrically prepared high purity standard solutions. Along with aerosol samples, procedural as well as field filter blanks were analyzed for the cations and anions. Subsequently, the sample signals were corrected for the field blanks. Based on the repeat analyses of working standard solutions, the concentrations of NO_3^- and NH_4^+ measured on the Ion chromatograph are reproducible within 5% for this dataset (Bikkina et al. (2020). Additionally, the commercially procured standard solution showed well agreement within 10% on the calibrations performed with working standard solutions.

Another 10 cm^2 filter cut of the TSP sample was extracted with ultrapure deionized water by ultrasonic agitation and filtered through the 0.22 µm disc filter (PVDF, Milex-GV). This filtrate was analyzed for WSTN on the total nitrogen (TN) analyzer (Shimadzu model, TOC-VCSH+TNM-1) by detecting it as NO_x with a chemiluminescence detector (Nakamura et al., 2006). The TN analyzer was calibrated with gravimetrically prepared ammonium nitrate standard solutions. Additionally, we analyzed two independent organic nitrogen standard solutions (Urea: 3.5 ppm-N and L-Aspartic acid: 0.4 ppm-N) on the TN analyzer. The measured WSTN from the urea and L-aspartic acid standard solutions yielded an external precision of 10.9% and 2.8%, respectively. The oxidation efficiency of organic nitrogen by the TN analyzer was 89-97% for our study. The concentrations of WSON is obtained by subtracting the inorganic nitrogen (WSIN = $NH_4^+ + NO_3^-$) from the WSTN. We defined the method detection limits (MDL) as the three times the standard deviation of field blank levels normalized to the average air volume filtered through the aerosol sample (~1642 m^3). The MDLs for NO_3^-, NH_4^+ and WSTN are ascertained as 1.6, 3.4 and 1.2 nmol m^{-3}, respectively. The field blanks contribute from 17% to less than 1% of signal observed for the aerosol NO_3^- and NH_4^+ respectively. Likewise, the field filter blanks contribute to 2.8% to 0.2% of signal observed for the WSTN concentrations of aerosols collected over the Arabian Sea.

2.3. Error propagation in N_{org} concentrations

We calculated WSON as difference in concentrations of WSTN and WSIN, which are from the two different analytical instruments. In such a scenario, the subtracting the contribution of two large numbers to derive $N_{Org\text{-}WS}$, thereby, associated with considerable uncertainties (Mace and Duce, 2002; Cornell et al., 2003). If in an aerosol, the WSIN dominates the WSTN, then the estimated WSON is associated with relatively large uncertainty and in some cases yields a negative concentration. Several studies have addressed the potentially large uncertainty arising with the estimates of WSON due to rounding negative numbers to zero and, hence, leading to the overestimation of WSON reported by earlier studies (Mace et al., 2003a; Mace et al., 2003b; Lesworth et al., 2010). Therefore, we discarded any of the large negative values of WSON similar to the approach adopted by Lesworth et al. (2010). This criterion allows us to exclude one sample (sample id: SS379#3 collected on 8 Deceember 2018) for estimating the WSON. Besides, we chose to exclude all those measurements in which propagated errors of WSON are comparable or larger than its concentration estimated by the difference in WSTN and WSIN. We used the external precision of 5% on NH_4^+ and NO_3^- as well as 10% for WSTN in TSP samples in a Monte Carlo error propagation method (MCEP; (Spiess, 2018)) for estimating the uncertainties of WSON (Bikkina et al., 2020).

Other supporting chemical composition data on carbonaceous components including water-soluble organic carbon (WSOC), elemental and organic carbon (EC and OC) as well as other major inorganic ions (viz., K^+, SO_4^{2-}) were obtained from our recent publication (Bikkina et al., 2020). Briefly, a 16 mm diameter filter punch of TSP was analyzed for EC and OC using the national institute for occupational safety and health (NIOSH5040) protocol on the sunset carbon analyzer (Sunset Laboratory, SF, CA). Here, the instrument performance was assessed with the potassium hydrogen phthalate standard solution and found that total carbon measurements agreed within ~5%. Moreover, EC was not detected in field blanks and OC signal was centered on ~2.0 μg cm^{-2}, which contributes to only 20% of the minimum signal measured in TSP samples. For the detailed extraction procedure for OC/EC analysis, please refer to Boreddy and Kawamura (2015) and Bikkina et al. (2020).

3. Results and discussion

3.1. Concentrations and relative abundances

The temporal variability of concentrations of aerosol-N is governed by the source strength of emissions, dilution of air parcels and chemical processes occurring during transport (Jickells, 2006). We found that the concentrations of WSIN and WSON in the TSP samples showed pronounced temporal variability (Table 1). In general, concentration of NH_4^+ in the aerosols over the Arabian Sea (18-324 nmol m^{-3}; 109±82 nmol m^{-3}) exceeded that of NO_3^- (13-62 nmol m^{-3}; 32±13 nmol m^{-3}) during winter. Likewise, the concentrations ranged from 53 to 451 nmol m^{-3} (220±92 nmol m^{-3}) for WSTN and 0 to 263 nmol m^{-3} (86±81 nmol m^{-3}) for WSON during winter. We compared the average loadings of aerosol-N species over the Arabian Sea from the present study with those reported over other oceans (Table 2).

A comparison of concentration of WSIN in ambient aerosols collected over the Arabian Sea are somewhat comparable with the present study (140±83 nmol m^{-3} (this study); 100 nmol m^{-3}; (Krishnamurti et al., 1998); 147±100 nmol m^{-3} (Kumar et al., 2012); 91±12 nmol m^{-3} (Aswini et al., 2020)) but higher than those obtained from the spring (36±13 nmol m^{-3} (Johansen et al., 1999) and summer (10±3 nmol m^{-3} (Johansen et al., 1999)) seasons. This is because of the combined influence of the entrapment of anthropogenic source-emissions within the shallow boundary layer height and strong northeastern monsoonal winds during winter (Jayaraman et al., 1998; Ramanathan et al., 2001; Nair et al., 2007; Bosch et al., 2014). Furthermore, the concentrations of WSIN over the Arabian Sea during winter season (this study) are also similar to those documented over the Bay of Bengal (Table 2), which is attributable to the impact of continental outflow from similar source-

emissions in the Indo-Gangetic Plain (Bikkina et al., 2011). Likewise, the concentrations of WSIN from the Arabian Sea are also comparable to those obtained from other island-based receptor sites such as those from Ireland, Mace Head; (Spokes et al., 2000) but higher than those observed over Hawaii (Cornell et al., 2001; Carrillo et al., 2002) and the East China Sea (Chen et al., 2010). Likewise, the average concentrations of WSON over the Arabian Sea are somewhat comparable to those observed over the Bay of Bengal (59±54 nmol m^{-3}; (Bikkina et al., 2011)), South China Sea (65±20 nmol m^{-3}; (Shi et al., 2010)), Yellow Sea (87 nmol m^{-3}; (Shi et al., 2010)), and East China Sea (54±36 nmol m^{-3}; (Nakamura et al., 2006)). But the mean concentration of WSON over the Arabian Sea (this study) is higher than those reported over the Pacific Ocean (16±19 nmol m^{-3}; (Nakamura et al., 2006); 29±25 nmol m^{-3}; (Cornell et al., 2001)), Atlantic Ocean (9.8 nmol m^{-3}; (Lesworth et al., 2010)). Besides, the concentrations of WSON over the Arabian Sea (this study) are also comparable to those for the biomass burning emissions in the Indo-Gangetic Plain (Kharagpur: 96±63 nmol m^{-3}; (Bikkina et al., 2015)) but higher than those over other European (Erdemli, Turkey: 29±42 nmol m^{-3}; (Mace et al., 2003b)) and US urban sites (Davis, California: 19±14 nmol m^{-3}; (Zhang et al., 2002)).

3.2. Source apportionment

To ascertain the possible sources of aerosol-N over the Arabian Sea due to long-range transport from South Asia, we have examined the latitudinal variability of NH_4^+, NO_3^- and WSON along with anthropogenic (*e.g.* nss-SO_4^{2-}, nss-K^+, nss-Ca^{2+}, WSOC, OC, and EC) and marine (*e.g.* Na^+, methanesulfonic acid: MSA) chemical tracers. We observed a close resemblance in the latitudinal variability of NH_4^+, nss-SO_4^{2-} and nss-K^+ (Figure 2a, g, h). Likewise, there is a similar latitudinal variability between NO_3^- and nss-Ca^{2+} (Figure 2b, i). In addition, there is similar latitudinal variability of WSON concentrations with WSOC, OC and EC (Figure 2c-f). In contrast, no similarity persists between measured aerosol-N species (Figure 2a-c) and marine biogenic tracers (Figure 2j-k). Subsequently, we have examined the strength of the linear correlations between aerosol-N species and anthropogenic tracers.

Open burning of post-harvest crop-residues and domestic wood-fuel combustion in the Indo-Gangetic Plain (IGP) is a major source of water-soluble K^+ in ambient aerosols (Zhang et al., 2013; Bikkina and Sarin, 2014; Rajput et al., 2014). Recently, PM_{10} samples (*i.e.*, particles having aerodynamic diameter <10 μm) collected from the field burns of rice and maze straw in the Chiang Mai Province, Thailand, showed high concentrations of K^+, NH_4^+ and NO_3^- (Sillapapiromsuk et al., 2013). We observed a strong correlation between NH_4^+ and nss-K^+ in TSP samples (Figure 3a),

suggesting their contribution from biomass burning emissions. Backward air mass trajectories for the sampling days of TSP over the Arabian Sea further originated from the IGP and intercepted by the MODIS fire counts within this provenance. However, the IGP is also a perennial source of NH_3 because of the emissions from crop-fields (i.e., where the widespread use of fertilizers, e.g., Urea) and animal husbandry. Parashar et al. (1998) estimated that NH_3 in ambient air in India is mainly originate from the fertilizer (1175 Gg), animal livestock (1433 Gg) and biomass burning (50 Gg). Therefore, we attribute the observed positive linear correlation between NH_4^+ and nss-K^+ to their common source-emissions and/or transport history.

The NH_4^+ in the atmosphere mostly exists in fine mode aerosols as ammonium sulphate or ammonium bisulphate (NH_4HSO_4). Accordingly, we observed a strong positive linear relationship between molar concentrations of NH_4^+ and SO_4^{2-} (Bikkina et al., 2020) with a regression slope of ~1.8, suggesting the presence of this aerosol-N species in fine mode.

$$NH_3 + H_2SO_4 \rightarrow NH_3HSO_4 \text{ or } (NH_4)_2SO_4 \quad (1)$$

The NO_3^- in atmospheric aerosols usually originated by the reaction of nitric acid with major alkaline species (NH_3, dust and sea salts) (Song and Carmichael, 2001; Jickells, 2006). Here, nitric acid is an oxidation product of NO_x, which is mostly emitted by the fossil fuel combustion sources, however, biomass burning also significantly contributes to NO_x emissions (Yeatman et al., 2001; Seinfeld and Pandis, 2016). A canonical representation of NO_3^- aerosol formation by these processes can be explained by the following chemical reactions.

$$NH_3 + HNO_3 \leftrightharpoons NH_4NO_3 \quad (2)$$

$$CaCO_3 \text{ (dust)} + HNO_3 \rightarrow Ca(NO_3)_2 \quad (3)$$

$$NaCl \text{ (sea salt)} + HNO_3 \rightarrow NaNO_3 \quad (4)$$

Studies on the size distribution of aerosol NO_3^- over the world oceans, influenced by the continental pollution sources such as the western North Pacific, Bay of Bengal, Atlantic and Mediterranean Sea, have revealed its predominant coarse nature in marine aerosols (Zhuang et al., 1999; Yeatman et al., 2001; Jordan et al., 2003; Galindo et al., 2008; Bikkina et al., 2011). This is because of the heterogeneous reactive uptake of gaseous or condensed phase of nitric acid in the atmosphere on to a pre-existing coarse mode mineral and/or sea salt aerosol (Eqn 3-4). There was no significant linear relationship observed between NH_4^+ and NO_3^- (Figure S1b). However, NO_3^- moderately correlated with nss-Ca^{2+}, dust tracer (Rastogi and Sarin, 2006; Tyagi et al., 2016)) in marine aerosols over the Arabian Sea (Figure 3b), suggesting the association of NO_3^- with the

mineral dust during transport. We could not observe any significant relation between NO_3^- and Na^+ (a tracer for sea salt) confirming absence of marine source. A strong positive linear relationship is observed between Na^+ and Mg^{2+} in the TSP during winter with slope comparable to weight ratio of Mg^{2+}/Na^+ in seawater (0.12;(Bikkina et al., 2020)) confirming that Na^+ in the TSP samples is mostly derived from seawater. Therefore, a lack of correlation between NO_3^- and Na^+ in the aerosols collected over the Arabian Sea suggests the minor role of heterogeneous formation of nitrate on sea-salt aerosols.

The WSON was strongly correlated with WSOC (Figure 3c), OC (Figure 3d) and EC (Figure 3e) over the Arabian Sea, implying its origin from anthropogenic combustion sources. Here, one sample has high OC loading (SS379#16 has OC beyond 99.9% percentile of the data) and the highest contribution from secondary formation processes (~61% of OC is secondary origin; Bikkina et al. 2020). Therefore, we excluded this TSP sample from the regression (see the black square in Figure 3c) analysis. The OC/EC (2.5-10.5) and WSOC/OC (0.30-0.74) ratios from this study are comparable to those observed for the biomass burning source regions in the IGP (OC/EC: 6.5±1.9; WSOC/OC: 0.69±0.09; (Rastogi et al., 2014)). Therefore, the observed strong correlations of WSON with WSOC, OC and EC in marine aerosols highlight the contribution from biomass burning emissions. However, other major source-emissions including fertilizers (*e.g.* Urea) and animal husbandry also contribute to WSON over the IGP. Therefore, the WSON in marine aerosols over the Arabian Sea can have mixed contributions from biomass burning, fertilizer use and animal livestock emissions.

3.3. Relative abundances

Compared to NH_4^+, NO_3^- is a minor contributor to the WSIN mass loading, however, the molar ratios of NO_3^-/WSIN are somewhat higher over 15-24 °N (0.10-0.68; av. 0.40) than over 5-15 °N (0.08-0.48; av. 0.21; Figure 4a). In contrast, NH_4^+/WSIN showed higher values over the low latitudes (5-15 °N: 0.52-0.92; av. 0.79) than those observed over high latitudes (15-24 °N; 0.32-0.90; av. 0.60; Figure 4b) indicate the contribution from biomass burning is a major source of ambient NH_3. Since the NH_4^+ concentration dominates the mass loadings of WSIN, a similar latitudinal distribution of WSIN/WSTN with NH_4^+/WSIN further highlights the significance of this aerosol-N species as a nutrient in the wintertime continental outflow. These latitudinal trends reflecting their variable source influence of constituent species of WSIN from biomass burning emissions and fossil-fuel combustion sources. NO_3^- in aerosols originates from the oxidation of NO_x emitted mostly by the vehicular emissions but also to some extent can be emitted from biomass burning.

The fractional contribution of WSON/WSTN also exhibited higher values over 15-24 °N than those observed over 5-15 °N. A close examination of the spatial variability of WSTN along with all the contributing aerosol-N components over the Arabian Sea (Figure 5) has revealed contrasting trends for NH_4^+ and WSON. To understand the influence of long-range transport of biomass burning emissions in South Asia on the atmospheric abundances of WSTN, we have examined the moderate resolution imaging spectroradiometer (MODIS) based fire counts and backward air mass trajectories during our study period. It is clear from Figure 6 that backward air mass trajectories during the sampling days not only originate from northwestern IGP and southern India but also intercepting the fire counts within this provenance. We have previously observed that the OC/EC ratios are higher (6-10) for the TSP samples collected over 18-24 °N (4.4-10.5; av. 5.9) and 7-10 °N (5.7-6.3; av. 5.98) over the Arabian Sea than those over 10-18 °N (2.5-4.6; av. 3.8) (Bikkina et al., 2020). Several field studies have shown that OC/EC ratios from biomass burning emissions are higher than those from the fossil-fuel combustion (Neusüß et al., 2002; Rengarajan et al., 2007; Sudheer and Sarin, 2008; Rajput et al., 2011; Ram and Sarin, 2011; Bikkina and Sarin, 2014; Aswini et al., 2020). Therefore, observed differences in the N-S gradient in the WSON/WSTN and WSIN/WSTN over the Arabian Sea (Figure 5) are, perhaps, due to the influence from the biomass burning sources in the northwestern IGP and southern India, respectively.

3.4. Air-to-Sea deposition – biogeochemical significance

3.4.1. Dry-deposition fluxes

In this study, the dry-deposition fluxes (f_{dry}) of aerosol-N species were assessed by the concentration times the dry-deposition velocity (V_{dry})

$$f_{\text{dry-aerosol-N}}\ (\mu\text{mol m}^{-2}\ \text{d}^{-1}) = [\text{N}]_{\text{aero}} \times V_{\text{dry}} \qquad (5)$$

In Eqn 5, $[N]_{aero}$ is the concentrations of NH_4^+, NO_3^-, and WSON over the Arabian Sea. The V_{dry} values, in general, depend on several environmental factors including wind speed, terrain roughness, and particle size. However, V_{dry} is experimentally measured based on the wind-tunnel experiments in the literature and very difficult to perform for all geographical locations. Consequently, most of the studies focusing on dry-deposition fluxes of reactive nitrogen use model-predicted dry-deposition velocities of coarse and fine mode particles as 1.0 cm s^{-1} and 0.1 cm s^{-1}, respectively (Duce et al., 1991; Baker et al., 2003; Bikkina et al., 2011). The simultaneous collection of $PM_{2.5}$ and PM_{10} (*i.e.*, particles having an aerodynamic diameter of <2.5 and 10 µm, respectively) over the Bay of Bengal during winter revealed the differences in the size-distributions of aerosol-N species. We observed that NO_3^- tends to exist in coarse mode (high concentrations for >2.5-10 µm), whereas NH_4^+ and

WSON are preferentially enriched in fine mode aerosols (high concentrations for <2.5 μm particles) over the Bay of Bengal in winter. As the wind regimes over the Arabian Sea during our study period are similar to that observed over the Bay of Bengal, it is reasonable to assume that aerosol-N species have similar size distributions. Therefore, we used V_{dry} of 1.0 cm s^{-1} for NO_3^- and 0.1 cm s^{-1} for NH_4^+ and WSON.

The dry-deposition fluxes of NH_4^+, NO_3^- and WSON over the Arabian Sea in winter varied from 1.6 to 28 μmol m^{-2} d^{-1} (9.4±7.1 μmol m^{-2} d^{-1}), 11 to 53 μmol m^{-2} d^{-1} (27±11 μmol m^{-2} d^{-1}), and 0 to 23 μmol m^{-2} d^{-1} (7.4±7.0 μmol m^{-2} d^{-1}), respectively. The estimated WSTN deposition flux ($f_{dry-WSTN}$) averages around 44±15 μmol m^{-2} d^{-1} (21-73 μmol m^{-2} d^{-1}) into the Arabian Sea are comparable to those observed during winter in the Bay of Bengal (2.1-127 μmol m^{-2} d^{-1}; 38±34 μmol m^{-2} d^{-1} (Bikkina and Sarin, 2013)).

We approximated the wet deposition fluxes of aerosol nitrogen using the approach of Duce et al. (1991).

$$f_{wet}\ (\mu mol\ m^{-2}\ d^{-1}) = P * S * C_{aero} * \rho_{water}/\rho_{air} \qquad (6)$$

Here, P is the precipitation rate; S is the scavenging ratio and C_{aero} is the concentration of aerosol-N.

P is considered as <3.0 mm d^{-1}, which is obtained from the tropical rainfall measurement mission (TRMM) archived datasets in the Giovanni data portal (https://giovanni.gsfc.nasa.gov/giovanni/). Bange et al. (2000) used 780 mm yr^{-1} (or 2 mm d^{-1}) for estimating the wet-deposition flux of aerosol nitrogen to the Arabian Sea. Since the TRMM retrieved precipitation rate overlaps with that of Bange et al. (2000), we used P = 2 mm d^{-1} for calculating the f_{wet} of WSIN over the Arabian Sea. The term S is basically the concentration ratio of nitrogen species in water to that in air. Duce et al. (1991) suggested somewhat high scavenging ratio for nitrate because of the coarse mode association with sea salt or mineral dust (*i.e.*, precipitation efficiently scavenges bigger particles) and low ratio for NH_4^+ due to the fine mode occurrence as $(NH_4)_2SO_4$ and/or NH_4HSO_4 aerosol. To be consistent with earlier approaches, we have also adopted here S = 330 for NO_3^- and S = 200 for NH_4^+ (Singh et al., 2012). It is worth mentioning that the data on scavenging ratios in the literature is only available for WSIN and, therefore, we could not constrain the f_{wet} for WSON using the proposed approach of Duce et al. (1991). Likewise, ρ_{air} and ρ_{water} are the densities of air (1.2 kg m^{-3}) and water (1000 kg m^{-3}), respectively. Using the average concentrations of aerosol NO_3^- (32 nmol m^{-3}) and NH_4^+ (109 nmol m^{-3}) over the Arabian Sea, their estimated wet-deposition fluxes were 17.6 and 36.3 μmol m^{-2} d^{-1}, respectively. However, no precipitation events

were recorded during the cruise in the Arabian Sea. This means that the f_{dry} dominates total atmospheric deposition (*i.e.*, f_{wet} is highly uncertain and indirect estimate from the aerosol-N) over the Arabian Sea during the study period, which is mainly because of the lesser rainfall amount received by the basin.

The combined estimate of average dry-deposition flux of WSTN (44 μmol m^{-2} d^{-1}) and wet-deposition of WSIN (53 μmol m^{-2} d^{-1}) to the Arabian Sea during our winter cruise has been integrated for an area covered by the SS379 cruise track (1.03×10^{12} m^2) and for the duration of the continental outflow (~150 days; late November to early April). This calculation has yielded a total air-to-sea deposition of 0.21 Tg-N yr^{-1}, which is somewhat lower than the previous estimate of Singh et al. (2012) for this marine basin (1.39 Tg-N yr^{-1}). This is because of the larger area (4.93×10^{12} m^2) and also higher deposition velocity (1.5 cm s^{-1}) wese used for NO_3^- in the Singh et al. (2012). It is also worth noting that the concentrations of WSIN from our study are reasonably comparable with the other cruises conducted in the Arabian Sea (*i.e.*, their tracks also covered most of the open ocean waters; Table 2). We, therefore, presumed that similar concentration levels for the WSTN prevail in the entire marine boundary layer of the Arabian Sea during the continental outflow. In such scenario, the estimated atmospheric total deposition flux of WSTN for the entire Arabian Sea is about 1.02 Tg-N yr^{-1}, which is comparable to the previous estimate of 1.39 Tg-N yr^{-1} by (Singh et al., 2012). However, we need real-time wet deposition fluxes to evaluate this budget due to the prevailing uncertainties associated with the scavenging ratios of aerosol-N from another site and the precipitation data from the satellites. To assess the role in marine productivity in the surface waters of the Arabian Sea, it is a prerequisite to compare these air-to-sea deposition fluxes of WSTN ($f_{dry\text{-}WSTN}$) with the other external nitrogen sources (*e.g.* riverine supply). We have estimated the riverine supply of total dissolved nitrogen flux to the Arabian Sea.

3.4.2. Comparison with riverine supply

The Arabian Sea receives lesser freshwater discharge from the peninsular rivers (Indus, Narmada, Tapi, Mahi, Sabarmati, Vishwamitiri, and Mandovi) as compared to the eastern counterpart of the northern Indian Ocean, the Bay of Bengal. On an average, the freshwater efflux per annum to the Arabian Sea is ~0.34×10^{12} m^3 yr^{-1} (Indus: 238×10^9 $m^3 yr^{-1}$; Narmada: 47×10^9 m^3 yr^{-1}; Tapi: 19×10^9 $m^3 yr^{-1}$; Mahi: 12×10^9 $m^3 yr^{-1}$; Sabarmati: 4×10^9 $m^3 yr^{-1}$; Vishwamitiri: 1×10^9 $m^3 yr^{-1}$; Mandovi: 16×10^9 $m^3 yr^{-1}$) (Bikkina and Sarin, 2013)). Kumar et al. (1996) estimated the total dissolved nitrogen load to the Bay of Bengal using the freshwater discharge to this marine basin and the global freshwater discharge data (37.4×10^{12} m^3 yr^{-1}); (Martin and Whitfield, 1983)) and

nitrogen load by the world rivers (50 Tg yr^{-1}; (Duce et al., 1991)). A similar strategy was employed here to derive the total dissolved nitrogen flux to the Arabian Sea (0.45 Tg yr^{-1}; this study). It is worth mentioning that the approach undertaken here has limitations because of the inherent uncertainty associated with global and regional riverine discharge flux as well as the soluble nitrogen load from the peninsular rivers. We, therefore, acknowledge that ours is a preliminary attempt to constrain how much is the fluvial input of water-soluble nitrogen species relative to the estimated atmospheric dry-deposition flux of WSTN to the Arabian Sea and require future assessment along this line. Moreover, it is not obvious from this estimate that how much is the contribution from inorganic versus organic nitrogen components. While many studies reported the concentrations of inorganic nitrogen from the marine aerosols and the peninsular rivers, there were only few studies about the WSON.

Growing body of the literature have pointed out the bioavailability of WSON in the atmospheric aerosols as an important nutrient for the surface waters (Kanakidou et al., 2012; Xu et al., 2017; Matsumoto et al., 2018; Matsumoto et al., 2019; Djaoudi et al., 2020; Chen and Huang, 2021). Anthropogenic activities involving the secondary organic nitrate formation, extensive use of urea as a fertilizer for the Indian crops, significantly contribute to the continental outflows (Pavuluri et al., 2010; Bikkina et al., 2011; Bikkina and Sarin, 2013). In comparison to the datasets reporting on WSIN in aerosols, studies on organic component is rather limited for the northern Indian Ocean. Thus, we need more measurements to constrain the relative contributions of inorganic and organic nitrogen deposition to the downwind surface waters. Using the real-time datasets of dissolved organic nitrogen, recently Krishna et al. (2015) have estimated that the Arabian Sea receives ~0.11 Tg-N yr^{-1} by the peninsular rivers. Besides, Krishna et al., (2016) have documented that fluvial input of dissolved inorganic nitrogen (*i.e.,* analog of WSIN) to the Arabian Sea as 0.10 Tg-N yr^{-1}. This means the total dissolved nitrogen load from the Indian monsoonal rivers is about 0.21 Tg-N yr^{-1} (Krishna et al., 2015; Krishna et al., 2016). We translated the dry-deposition fluxes of WSON ($f_{dry\text{-}WSON}$) to the Arabian Sea (4.93×10^{12} m^2) for the duration of the continental outflow (*i.e.*, ~150 days; spanning from late November to early April; (Bikkina and Sarin, 2013)). This calculation yielded an air-to-sea deposition flux of WSON as high as 0.24 Tg yr^{-1} (av. 0.077 Tg yr^{-1}). Our estimated average dry-deposition flux of WSON to the Arabian Sea, thus, contributes to ~70% of dissolved organic nitrogen supply from the peninsular rivers (Figure 6).

3.4.3. Relevance to primary productivity by phytoplankton

To assess the influence of atmospheric dry-deposition of WSTN on the primary productivity in the surface waters of the Arabian Sea, a pseudo approximation has been made such that other

external N-sources are only minor contributors. In such a scenario, atmospheric dry-deposition fluxes of soluble nitrogen could serve as a major source to the surface waters and can thrive phytoplankton primary productivity (Spokes et al., 2000). Until recently, the role of dissolved organic nitrogen as a source of nutrients has been largely neglected and only highlighted the role of inorganic nitrogen species in the surface waters. Recent studies have shown that almost all parts of dissolved nitrogen (including inorganic and organic species) in the surface waters are bioavailable and, thus, support primary productivity (Seitzinger et al., 2002; Bronk et al., 2007; Sarma et al., 2019; Shetye et al., 2019).

In the euphotic waters, marine phytoplankton assimilate dissolved CO_2 into organic carbon by consuming relatively constant proportion of nutrients (based on a Redfield ratio; C:N:P = 106:16:1; (Redfield, 1963)). This means for every mole of dissolved N, there are 6.625 moles of C fixed (Spokes et al., 2000). Therefore, we converted the estimated atmospheric dry-deposition fluxes of WSTN (21-73 µmol-N m^{-2} d^{-1}; Figure 6) into equivalent carbon fluxes (139-484 µmol-C m^{-2} d^{-1}) using the Redfield stoichiometry. Furthermore, these estimated fluxes (1.7-5.8 mg-C m^{-2} d^{-1}) are compared with the net primary productivity measurements from the winter season (200-606 mg-C m^{-2} d^{-1};(Gauns et al., 2005); 110-200 mg-C m^{-2} d^{-1} (Bhattathiri et al., 1996)). This comparison revealed that atmospheric dry-deposition of WSTN can support at most 5.3% of water-column primary productivity in the Arabian Sea. Furthermore, air-to-sea deposition of WSTN essentially contributes to new nitrogen reservoir in the surface waters (*i.e.*, recycled-N + upwelled-N+ aerosol-N) (Duce et al., 2008)). Therefore, it is also important to estimate how much of the aerosol-N deposition contribute to new production in the Arabian Sea. The mean ratio of new-N to total dissolved N pool (*aka f*-ratio) is ranged between 0.14 and 0.82 with mean of 0.3 (Watts and Owens, 1999). Based on mean *f*-ratio of 0.3 in the Arabian Sea, the mean atmospheric N deposition (44±15 µmol-N m^{-2} d^{-1} ≈ 3.5±1.2 mg-C m^{-2} d^{-1}; assuming Redfield ratio) could support on an average 10.6±1.2% of the new production in the Arabian Sea.

The coastal waters receive external nutrients from submarine ground water discharge (SGD), river discharge and atmospheric deposition. The SGD occurs along the west coast of India (>7500 km) and it is relatively higher in the southwest and northwest coast than central region. Recently Kumar et al. (2020) estimated dissolved inorganic nitrogen flux to the west coast of India through SGD to be 0.06±0.03 Tg-N yr^{-1}. Likewise, Krishna and coworkers have estimated that Indian monsoonal rivers contribute ~0.11±0.02 Tg-N yr^{-1} of dissolved organic nitrogen (i.e., analog of WSON; (Krishna et al., 2015)) and 0.10±0.02 Tg-N yr^{-1} of dissolved inorganic nitrogen (i.e., analog of WSIN; (Krishna et al., 2016)) to the coastal Arabian Sea. This external inorganic and/or organic

nitrogen inputs to the Arabian Sea are comparable to the atmospheric dry-deposition of WSON to the Arabian Sea based on the mean and maximum aerosol concentrations correspond to 0.077 and 0.24 Tg-N yr^{-1}, respectively during the period of continental flow. The contribution of atmospheric deposition of WSTN (1.0 Tg-N yr^{-1}) is estimated to be 79% whereas SGD and river discharge accounts to 5 and 16% to the external sources of dissolved nitrogen to the coastal Arabian Sea. All these external sources not only increase concentration of nutrients but also modify stoichiometry of the nutrients, which may have significant impact on composition of plankton. Further studies are required to evaluate the impact of deposition of atmospheric pollutants on plankton diversity in the coastal waters.

4. Summaries and future research directions

The wintertime aerosols collected over the Arabian Sea during the impact of pronounced continental outflow from South Asia have revealed abundant presence of NH_4^+ and WSON. This is in sharp contrast to previous observations where the importance of NO_3^- was highlighted (Kumar et al., 2008). One plausible explanation for the discrepancy is that previous observations from the Kumar et al. (2008) are mostly from the Spring-intermonsoon season, which is a transition period with a rather weak influence from the pollution sources in South Asia. We observed a significant positive linear relationship of WSON with WSOC as well as NH_4^+ with nss-K^+, suggesting their likely contribution from biomass burning emissions along with other sources (fertilizer use, animal husbandry). This inference was further supported by the backward air mass trajectories and MODIS fire counts that altogether highlight the contribution of WSON from the biomass burning emissions in northwestern IGP and southern India over the Arabian Sea. Besides, the maximum dry-deposition fluxes of WSON are of comparable magnitude with that of riverine supply. This observation is, thus, highlighting the significance of atmospheric route of this major nutrient to the downwind surface waters of the Arabian Sea.

Given the comparable source strength of atmospheric and riverine inputs of dissolved organic nitrogen to the Arabian Sea, it is important to understand the extent of labile and refractory pools, as well as their exchange between particulate/colloidal phases. Furthermore, it is also important to assess the relative and combined roles of dry deposition of organic nitrogenous species with NH_4^+ in influencing the phytoplankton primary productivity in the surface waters. Likewise, we need simultaneous aerosol sampling along with the measurements of water-column primary productivity to further underpin the real-time significance of the atmospheric deposition of aerosol-N on the surface ocean biogeochemistry.

Acknowledgements

PB acknowledges the partial financial support from the DST-INSPIRE fellowship (DST/INSPIRE/04/2017/000324 dated 24/07/2017) and JASSO (Japan Student Service Organization) Follow up research fellowship 2019. PB is grateful to the Scientist-In-Charge and the Director of NIO for the support at the workplace. PB and VVSS are thankful to the Ship Captain and crew for their support during the cruise. PB and VVSS Sarma acknowledge the support from the Chief Scientist Dr. GVM Gupta (CMLRE, Kochi) and Dr. CK Sherin on board of SS379 for their help in the sampling. KK acknowledges the financial support from Japan Society for the Promotion of Science (JSPS) under the Joint Research Program-LEAD (JRPs-LEAD with DFG). Authors thankfully acknowledge the NOAA Air Resources Laboratory for the access to the HYSPLIT model (http://www.arl.noaa.gov/ready.html). We also acknowledge NASA's Goddard Earth Sciences Data and Information Services Centre for providing access to MODIS fire count data from the GES-DISC Interactive Online Visualization and analysis portal. PB and SB acknowledge technical help from Dr. M.Y. Aslam Shareef in retrieving the precipitation rates from the tropical rainfall measurement mission (TRMM) data from the Giovanni Web portal. The NIO contribution number is xxxx.

References

Aswini, A.R., Hegde, P., Aryasree, S., Girach, I.A. and Nair, P.R., 2020. Continental outflow of anthropogenic aerosols over Arabian Sea and Indian Ocean during wintertime: ICARB-2018 campaign. Science of The Total Environment, 712: 135214.

Baker, A.R., Kelly, S.D., Biswas, K.F., Witt, M. and Jickells, T.D., 2003. Atmospheric deposition of nutrients to the Atlantic Ocean. Geophysical Research Letters, 30(24).

Bange, H.W. et al., 2000. A revised nitrogen budget for the Arabian Sea. Global Biogeochemical Cycles, 14(4): 1283-1297.

Bhattathiri, P. et al., 1996. Phytoplankton production and chlorophyll. Current Science, 71(11).

Bikkina, P. et al., 2020. Chemical characterization of wintertime marine aerosols over the Arabian Sea: Impact of marine sources and long-range transport. Atmospheric Environment: 117749.

Bikkina, S. and Sarin, M.M., 2013. Atmospheric deposition of N, P and Fe to the Northern Indian Ocean: Implications to C- and N-fixation. Science of The Total Environment, 456 - 457(0): 104-114.

Bikkina, S. and Sarin, M.M., 2014. PM2. 5, EC and OC in atmospheric outflow from the Indo-Gangetic Plain: Temporal variability and aerosol organic carbon-to-organic mass conversion factor. Science of The Total Environment, 487: 196-205.

Bikkina, S., Sarin, M.M. and Sarma, V.V.S.S., 2011. Atmospheric dry deposition of inorganic and organic nitrogen to the Bay of Bengal: Impact of continental outflow. Marine Chemistry, 127(1–4): 170-179.

Bikkina, S., Sarin, M.M. and Sarma, V.V.S.S., 2015. Atmospheric outflow of nutrients to the Bay of Bengal: Impact of anthropogenic sources. Journal of Marine Systems, 141: 34-44.

Boreddy, S. and Kawamura, K., 2015. A 12-year observation of water-soluble ions in TSP aerosols collected at a remote marine location in the western North Pacific: an outflow region of Asian dust. Atmospheric chemistry and physics, 15(11): 6437-6453.

Bosch, C. et al., 2014. Source - diagnostic dual - isotope composition and optical properties of water - soluble organic carbon and elemental carbon in the South Asian outflow intercepted over the Indian Ocean. Journal of Geophysical Research: Atmospheres, 119(20): 11,743-11,759.

Bronk, D.A., See, J.H., Bradley, P. and Killberg, L., 2007. DON as a source of bioavailable nitrogen for phytoplankton. Biogeosciences, 4(3): 283-296.

Cape, J., Cornell, S., Jickells, T. and Nemitz, E., 2011. Organic nitrogen in the atmosphere—Where does it come from? A review of sources and methods. Atmospheric Research, 102(1): 30-48.

Carrillo, J.H., Hastings, M.G., Sigman, D.M. and Huebert, B.J., 2002. Atmospheric deposition of inorganic and organic nitrogen and base cations in Hawaii. Global Biogeochemical Cycles, 16(4): 24-1-24-16.

Chen, H.-Y. et al., 2010. Size fractionation and molecular composition of water-soluble inorganic and organic nitrogen in aerosols of a coastal environment. Journal of Geophysical Research: Atmospheres, 115(D22).

Chen, H.-Y. and Huang, S.-Z., 2021. Composition and supply of inorganic and organic nitrogen species in dry and wet atmospheric deposition: Use of organic nitrogen composition to calculate the Ocean's external nitrogen flux from the atmosphere. Continental Shelf Research, 213: 104316.

Cornell, S., 2011. Atmospheric nitrogen deposition: revisiting the question of the invisible organic fraction. Procedia Environmental Sciences, 6: 96-103.

Cornell, S. et al., 2001. Organic nitrogen in Hawaiian rain and aerosol. Journal of Geophysical Research: Atmospheres, 106(D8): 7973-7983.

Cornell, S.E., 2014. Assessment and characterisation of the organic component of atmospheric nitrogen deposition, Nitrogen Deposition, Critical Loads and Biodiversity. Springer, pp. 107-116.

Cornell, S.E., Jickells, T.D., Cape, J.N., Rowland, A.P. and Duce, R.A., 2003. Organic nitrogen deposition on land and coastal environments: a review of methods and data. Atmospheric Environment, 37(16): 2173-2191.

Djaoudi, K. et al., 2020. Experimental evidence of the potential bioavailability for marine heterotrophic bacteria of aerosols organic matter. Biogeosciences Discuss., 2020: 1-24.

Doney, S.C. et al., 2007. Impact of anthropogenic atmospheric nitrogen and sulfur deposition on ocean acidification and the inorganic carbon system. Proceedings of the National Academy of Sciences, 104(37): 14580-14585.

Duce, R. et al., 2008. Impacts of atmospheric anthropogenic nitrogen on the open ocean. Science, 320(5878): 893-897.

Duce, R.A. et al., 1991. The atmospheric input of trace species to the world ocean. Global Biogeochemical Cycles, 5(3): 193-259.

Facchini, M.C. et al., 2008. Important Source of Marine Secondary Organic Aerosol from Biogenic Amines. Environmental Science & Technology, 42(24): 9116-9121.

Galindo, N. et al., 2008. Factors affecting levels of aerosol sulfate and nitrate on the Western Mediterranean coast. Atmospheric Research, 88(3): 305-313.

Gauns, M. et al., 2005. Comparative accounts of biological productivity characteristics and estimates of carbon fluxes in the Arabian Sea and the Bay of Bengal. Deep Sea Research Part II: Topical Studies in Oceanography, 52(14): 2003-2017.

Jayaraman, A. et al., 1998. Direct observations of aerosol radiative forcing over the tropical Indian Ocean during the Januaryâ€□February 1996 preâ€□INDOEX cruise. Journal of Geophysical Research: Atmospheres (1984â€“2012), 103(D12): 13827-13836.

Jickells, T., 2006. The role of air-sea exchange in the marine nitrogen cycle. Biogeosciences, 3(3): 271-280.

Jickells, T., Baker, A., Cape, J., Cornell, S. and Nemitz, E., 2013. The cycling of organic nitrogen through the atmosphere. Philosophical Transactions of the Royal Society B: Biological Sciences, 368(1621): 20130115.

Jickells, T.D. et al., 2017. A reevaluation of the magnitude and impacts of anthropogenic atmospheric nitrogen inputs on the ocean. Global Biogeochemical Cycles, 31(2): 289-305.

Johansen, A.M., Siefert, R.L. and Hoffmann, M.R., 1999. Chemical characterization of ambient aerosol collected during the southwest monsoon and intermonsoon seasons over the Arabian Sea: Anions and cations. Journal of Geophysical Research: Atmospheres, 104(D21): 26325-26347.

Jordan, C.E., Dibb, J.E., Anderson, B.E. and Fuelberg, H.E., 2003. Uptake of nitrate and sulfate on dust aerosols during TRACE-P. Journal of Geophysical Research: Atmospheres, 108(D21).

Kanakidou, M. et al., 2012. Atmospheric fluxes of organic N and P to the global ocean. Global Biogeochemical Cycles, 26(3).

Kanakidou, M. et al., 2016. Past, Present, and Future Atmospheric Nitrogen Deposition. Journal of the Atmospheric Sciences, 73(5): 2039-2047.

Krishna, M.S. et al., 2016. Export of dissolved inorganic nutrients to the northern Indian Ocean from the Indian monsoonal rivers during discharge period. Geochimica et Cosmochimica Acta, 172: 430-443.

Krishna, M.S. et al., 2015. Fluxes of dissolved organic carbon and nitrogen to the northern Indian Ocean from the Indian monsoonal rivers. Journal of Geophysical Research: Biogeosciences, 120(10): 2067-2080.

Krishnamurthy, A. et al., 2009. Impacts of increasing anthropogenic soluble iron and nitrogen deposition on ocean biogeochemistry. Global Biogeochemical Cycles, 23(3).

Krishnamurthy, A., Moore, J.K., Zender, C.S. and Luo, C., 2007. Effects of atmospheric inorganic nitrogen deposition on ocean biogeochemistry. Journal of Geophysical Research: Biogeosciences, 112(G2).

Krishnamurti, T., Jha, B., Prospero, J., Jayaraman, A. and Ramanathan, V., 1998. Aerosol and pollutant transport and their impact on radiative forcing over the tropical Indian Ocean during the January - February 1996 pre-INDOEX cruise. Tellus B, 50(5): 521-542.

Kumar, A., Sarin, M.M. and Sudheer, A.K., 2008. Mineral and anthropogenic aerosols in Arabian Sea–atmospheric boundary layer: Sources and spatial variability. Atmospheric Environment, 42(21): 5169-5181.

Kumar, A., Sudheer, A.K., Goswami, V. and Bhushan, R., 2012. Influence of continental outflow on aerosol chemical characteristics over the Arabian Sea during winter. Atmospheric Environment, 50: 182-191.

Kumar, B.S.K. et al., 2020. Spatial variations in dissolved inorganic nutrients in the groundwaters along the Indian coast and their export to adjacent coastal waters. Environmental Science and Pollution Research.

Kumar, M.D., Naqvi, S.W.A., George, M.D. and Jayakumar, D.A., 1996. A sink for atmospheric carbon dioxide in the northeast Indian Ocean. Journal of Geophysical Research: Oceans, 101(C8): 18121-18125.

Lesworth, T., Baker, A.R. and Jickells, T., 2010. Aerosol organic nitrogen over the remote Atlantic Ocean. Atmospheric Environment, 44(15): 1887-1893.

Lin, M., Walker, J., Geron, C. and Khlystov, A., 2010. Organic nitrogen in PM_{2.5} aerosol at a forest site in the Southeast US. Atmos. Chem. Phys., 10(5): 2145-2157.

Mace, K.A., Duce, R.A. and Tindale, N.W., 2003a. Organic nitrogen in rain and aerosol at Cape Grim, Tasmania, Australia. Journal of Geophysical Research: Atmospheres, 108(D11).

Mace, K.A., Kubilay, N. and Duce, R.A., 2003b. Organic nitrogen in rain and aerosol in the eastern Mediterranean atmosphere: An association with atmospheric dust. Journal of Geophysical Research: Atmospheres, 108(D10).

Mahowald, N.M. et al., 2017. Aerosol Deposition Impacts on Land and Ocean Carbon Cycles. Current Climate Change Reports: 1-16.

Marra, J. and Barber, R.T., 2005. Primary productivity in the Arabian Sea: A synthesis of JGOFS data. Progress in Oceanography, 65(2): 159-175.

Martin, J.-M. and Whitfield, M., 1983. The Significance of the River Input of Chemical Elements to the Ocean. In: C.S. Wong, E. Boyle, K.W. Bruland, J.D. Burton and E.D. Goldberg (Editors), Trace Metals in Sea Water. Springer US, Boston, MA, pp. 265-296.

Matsumoto, K., Sakata, K. and Watanabe, Y., 2019. Water-soluble and water-insoluble organic nitrogen in the dry and wet deposition. Atmospheric Environment, 218: 117022.

Matsumoto, K., Takusagawa, F., Suzuki, H. and Horiuchi, K., 2018. Water-soluble organic nitrogen in the aerosols and rainwater at an urban site in Japan: Implications for the nitrogen composition in the atmospheric deposition. Atmospheric Environment, 191: 267-272.

Matsumoto, K. et al., 2017. Origin of the water-soluble organic nitrogen in the maritime aerosol. Atmospheric Environment, 167: 97-103.

Miyazaki, Y., Fu, P., Ono, K., Tachibana, E. and Kawamura, K., 2014. Seasonal cycles of water-soluble organic nitrogen aerosols in a deciduous broadleaf forest in northern Japan. Journal of Geophysical Research: Atmospheres, 119(3): 1440-1454.

Miyazaki, Y., Kawamura, K., Jung, J., Furutani, H. and Uematsu, M., 2011. Latitudinal distributions of organic nitrogen and organic carbon in marine aerosols over the western North Pacific. Atmospheric Chemistry and Physics, 11(7): 3037-3049.

Miyazaki, Y., Kawamura, K. and Sawano, M., 2010a. Size distributions of organic nitrogen and carbon in remote marine aerosols: Evidence of marine biological origin based on their isotopic ratios. Geophysical Research Letters, 37(6).

Miyazaki, Y., Kawamura, K. and Sawano, M., 2010b. Size distributions of organic nitrogen and carbon in remote marine aerosols: Evidence of marine biological origin based on their isotopic ratios. Geophysical Research Letters, 37(6): n/a-n/a.

Mochizuki, T., Kawamura, K. and Aoki, K., 2016. Water-Soluble Organic Nitrogen in High Mountain Snow Samples from Central Japan. Aerosol and Air Quality Research, 16(3): 632-639.

Nair, V.S. et al., 2007. Wintertime aerosol characteristics over the Indo - Gangetic Plain (IGP): Impacts of local boundary layer processes and long - range transport. Journal of Geophysical Research: Atmospheres (1984‐2012), 112(D13): doi: 10.1029/2006JD008099.

Nakamura, T., Matsumoto, K. and Uematsu, M., 2005. Chemical characteristics of aerosols transported from Asia to the East China Sea: an evaluation of anthropogenic combined nitrogen deposition in autumn. Atmospheric Environment, 39(9): 1749-1758.

Nakamura, T., Ogawa, H., Maripi, D.K. and Uematsu, M., 2006. Contribution of water soluble organic nitrogen to total nitrogen in marine aerosols over the East China Sea and western North Pacific. Atmospheric Environment, 40(37): 7259-7264.

Naqvi, S.W.A. et al., 2005. Biogeochemical ocean-atmosphere transfers in the Arabian Sea. Progress in Oceanography, 65(2): 116-144.

Neusüß, C., Gnauk, T., Plewka, A., Herrmann, H. and Quinn, P.K., 2002. Carbonaceous aerosol over the Indian Ocean: OC/EC fractions and selected specifications from size-segregated onboard samples. Journal of Geophysical Research: Atmospheres, 107(D19): INX2 30-1-INX2 30-13.

Parashar, D.C., Kulshrestha, U.C. and Sharma, C., 1998. Anthropogenic emissions of NOX, NH3 and N2O in India. Nutrient Cycling in Agroecosystems, 52(2): 255-259.

Patra, P.K., Kumar, M.D., Mahowald, N. and Sarma, V.V.S.S., 2007. Atmospheric deposition and surface stratification as controls of contrasting chlorophyll abundance in the North Indian Ocean. Journal of Geophysical Research: Oceans, 112(C5).

Pavuluri, C.M., Kawamura, K., Tachibana, E. and Swaminathan, T., 2010. Elevated nitrogen isotope ratios of tropical Indian aerosols from Chennai: Implication for the origins of aerosol nitrogen in South and Southeast Asia. Atmospheric Environment, 44(29): 3597-3604.

Prospero, J.M., Ginoux, P., Torres, O., Nicholson, S.E. and Gill, T.E., 2002. Environmental characterization of global sources of atmospheric soil dust identified with the Nimbus 7 Total Ozone Mapping Spectrometer (TOMS) absorbing aerosol product. Reviews of geophysics, 40(1).

Qi, J.H., Shi, J.H., Gao, H.W. and Sun, Z., 2013. Atmospheric dry and wet deposition of nitrogen species and its implication for primary productivity in coastal region of the Yellow Sea, China. Atmospheric Environment, 81: 600-608.

Rajput, P., Sarin, M.M., Rengarajan, R. and Singh, D., 2011. Atmospheric polycyclic aromatic hydrocarbons (PAHs) from post-harvest biomass burning emissions in the Indo-Gangetic Plain: Isomer ratios and temporal trends. Atmospheric Environment, 45(37): 6732-6740.

Rajput, P., Sarin, M.M., Sharma, D. and Singh, D., 2014. Organic aerosols and inorganic species from post-harvest agricultural-waste burning emissions over northern India: impact on mass absorption efficiency of elemental carbon. Environmental Science: Processes & Impacts, 16(10): 2371-2379.

Ram, K. and Sarin, M.M., 2011. Day–night variability of EC, OC, WSOC and inorganic ions in urban environment of Indo-Gangetic Plain: Implications to secondary aerosol formation. Atmospheric Environment, 45(2): 460-468.

Ramanathan, V. et al., 2001. Indian Ocean Experiment: An integrated analysis of the climate forcing and effects of the great Indoâ€• Asian haze. Journal of Geophysical Research: Atmospheres (1984â€“2012), 106(D22): 28371-28398.

Rastogi, N. and Sarin, M.M., 2006. Chemistry of aerosols over a semi-arid region: Evidence for acid neutralization by mineral dust. Geophysical Research Letters, 33(23).

Rastogi, N., Singh, A., Singh, D. and Sarin, M., 2014. Chemical characteristics of PM2. 5 at a source region of biomass burning emissions: Evidence for secondary aerosol formation. Environmental Pollution, 184: 563-569.

Redfield, A.C., 1963. The influence of organisms on the composition of seawater. The sea, 2: 26-77.

Rengarajan, R., Sarin, M.M. and Sudheer, A.K., 2007. Carbonaceous and inorganic species in atmospheric aerosols during wintertime over urban and high-altitude sites in North India. Journal of Geophysical Research: Atmospheres, 112(D21): D21307.

Sarin, M.M., Rengarajan, R. and Krishnaswami, S., 1999. Aerosol NO-3 and 210Pb distribution over the central-eastern Arabian Sea and their air'sea deposition fluxes. Tellus B: Chemical and Physical Meteorology, 51(4): 749-758.

Sarma, V.V.S.S., Rao, D.N., Rajula, G.R., Dalabehera, H.B. and Yadav, K., 2019. Organic Nutrients Support High Primary Production in the Bay of Bengal. Geophysical Research Letters, 46(12): 6706-6715.

Seinfeld, J.H. and Pandis, S.N., 2016. Atmospheric chemistry and physics: from air pollution to climate change. John Wiley & Sons.

Seitzinger, S.P., Sanders, R.W. and Styles, R., 2002. Bioavailability of DON from natural and anthropogenic sources to estuarine plankton. Limnology and Oceanography, 47(2): 353-366.

Shetye, S.S. et al., 2019. Variability of organic nitrogen and its role in regulating phytoplankton in the eastern Arabian Sea. Marine Pollution Bulletin, 141: 550-560.

Shi, J., Gao, H., Qi, J., Zhang, J. and Yao, X., 2010. Sources, compositions, and distributions of water-soluble organic nitrogen in aerosols over the China Sea. Journal of Geophysical Research: Atmospheres, 115(D17).

Sillapapiromsuk, S., Chantara, S., Tengjaroenkul, U., Prasitwattanaseree, S. and Prapamontol, T., 2013. Determination of PM10 and its ion composition emitted from biomass burning in the chamber for estimation of open burning emissions. Chemosphere, 93(9): 1912-1919.

Singh, A., Gandhi, N. and Ramesh, R., 2012. Contribution of atmospheric nitrogen deposition to new production in the nitrogen limited photic zone of the northern Indian Ocean. Journal of Geophysical Research: Oceans, 117(C6).

Song, C.H. and Carmichael, G.R., 2001. Gas-Particle Partitioning of Nitric Acid Modulated by Alkaline Aerosol. Journal of Atmospheric Chemistry, 40(1): 1-22.

Spiess, A.-N., 2018. propagate: Propagation of Uncertainty. R package version 1.0-6. https://CRAN.R-project.org/package=propagate.

Spokes, L.J., Yeatman, S.G., Cornell, S.E. and Jickells, T.D., 2000. Nitrogen deposition to the eastern Atlantic Ocean. The importance of south-easterly flow. Tellus B: Chemical and Physical Meteorology, 52(1): 37-49.

Sudheer, A.K. and Sarin, M.M., 2008. Carbonaceous aerosols in MABL of Bay of Bengal: Influence of continental outflow. Atmospheric Environment, 42(18): 4089-4100.

Tindale, N.W. and Pease, P.P., 1999. Aerosols over the Arabian Sea: Atmospheric transport pathways and concentrations of dust and sea salt. Deep Sea Research Part II: Topical Studies in Oceanography, 46(8): 1577-1595.

Tyagi, P., Kawamura, K., Bikkina, S., Mochizuki, T. and Aoki, K., 2016. Hydroxy fatty acids in snow pit samples from Mt. Tateyama in central Japan: implications for atmospheric transport of microorganisms and plant waxes associated with Asian dust. Journal of Geophysical Research: Atmospheres: doi: 10.1002/2016JD025340.

Watts, L.J. and Owens, N.J.P., 1999. Nitrogen assimilation and the f-ratio in the northwestern Indian Ocean during an intermonsoon period. Deep Sea Research Part II: Topical Studies in Oceanography, 46(3): 725-743.

Wiggert, J.D., Hood, R.R., Banse, K. and Kindle, J.C., 2005. Monsoon-driven biogeochemical processes in the Arabian Sea. Progress in Oceanography, 65(2): 176-213.

Xu, W. et al., 2017. Seasonal Characterization of Organic Nitrogen in Atmospheric Aerosols Using High Resolution Aerosol Mass Spectrometry in Beijing, China. ACS Earth and Space Chemistry, 1(10): 673-682.

Yeatman, S.G., Spokes, L.J. and Jickells, T.D., 2001. Comparisons of coarse-mode aerosol nitrate and ammonium at two polluted coastal sites. Atmospheric Environment, 35(7): 1321-1335.

Zhang, Q., Anastasio, C. and Jimenez-Cruz, M., 2002. Water-soluble organic nitrogen in atmospheric fine particles (PM2.5) from northern California. Journal of Geophysical Research: Atmospheres, 107(D11): AAC 3-1-AAC 3-9.

Zhang, Y., Obrist, D., Zielinska, B. and Gertler, A., 2013. Particulate emissions from different types of biomass burning. Atmospheric Environment, 72: 27-35.

Zhu, L., Chen, Y., Guo, L. and Wang, F., 2013. Estimate of dry deposition fluxes of nutrients over the East China Sea: The implication of aerosol ammonium to non-sea-salt sulfate ratio to nutrient deposition of coastal oceans. Atmospheric Environment, 69: 131-138.

Zhuang, H., Chan, C.K., Fang, M. and Wexler, A.S., 1999. Formation of nitrate and non-sea-salt sulfate on coarse particles. Atmospheric Environment, 33(26): 4223-4233.

Table 1. Concentrations of water-soluble inorganic (WSIN≈NH_4^++NO_3^-) and organic nitrogen (WSON) in the total suspended particulate matter (TSP) collected over the Arabian Sea.

Sample id	date	#NH_4^+	#NO_3^-	#WSIN	#WSON	#WSTN	NH_4^+/WSIN	NO_3^-/WSIN	NH_4^+/WSTN	NO_3^-/WSTN	§WSON/WSTN
SS379_1	06-12-2018	22	21	43	11	53	0.52	0.48	0.41	0.39	0.20
SS379_2	07-12-2018	151	13	164	22	186	0.92	0.08	0.81	0.07	0.12
SS379_3	08-12-2018	324	36	360	b.d.	253	0.90	0.10	-	-	-
SS379_4	10-12-2018	111	37	149	22	171	0.75	0.25	0.65	0.22	0.13
SS379_5	11-12-2018	86	30	115	50	165	0.74	0.26	0.52	0.18	0.30
SS379_6	12-12-2018	91	24	115	30	146	0.79	0.21	0.63	0.17	0.21
SS379_7	13-12-2018	108	36	145	46	190	0.75	0.25	0.57	0.19	0.24
SS379_8	14-12-2018	104	27	131	20	150	0.80	0.20	0.69	0.18	0.13
SS379_9	15-12-2018	239	22	261	58	319	0.92	0.08	0.75	0.07	0.18
SS379_10	16-12-2018	170	19	188	263	451	0.90	0.10	0.38	0.04	0.58
SS379_11	17-12-2018	39	31	70	141	211	0.56	0.44	0.19	0.15	0.67
SS379_12	18-12-2018	18	21	39	140	179	0.47	0.53	0.10	0.12	0.78
SS379_13	19-12-2018	61	27	87	58	146	0.70	0.30	0.42	0.18	0.40
SS379_14	20-12-2018	152	46	198	61	259	0.77	0.23	0.59	0.18	0.24
SS379_15	21-12-2018	23	31	55	201	256	0.43	0.57	0.09	0.12	0.79
SS379_16	22-12-2018	125	62	187	107	294	0.67	0.33	0.43	0.21	0.36
SS379_17	23-12-2018	26	55	80	232	312	0.32	0.68	0.08	0.18	0.74

Note: Here # expressed in nmol m^{-3}; b.d. = below detection limits. §WSON/WSTN was considered "zero" for estimating the average percentage contribution for the dataset. Also - indicates that TSP sample has lower WSTN value by the TN analyzer than WSIN by the ion chromatograph.

Table 2. Comparison (nmol m^{-3}) of the atmospheric abundances and diagnostic mass ratios of water-soluble inorganic nitrogen (WSIN = NH_4^++NO_3^-) and organic nitrogen (WSON) in TSP samples collected over the Arabian Sea with those from other oceans.

Region	Duration	NH_4^+	NO_3^-	WSIN	WSON	NH_4^+/WSTN	NO_3^-/WSTN	WSON/WSTN	Reference
Arabian Sea	Dec'18	109±83	32±13	140±83	86±81	0.46±0.24	0.16±0.08	0.36±0.26	This study
Arabian Sea	Jan-Feb'96	73	27	-	-	-	-	-	Krishnamurti et al., 1998
Arabian Sea	Feb-Mar'95	-	39±16	-	-	-	-	-	Sarin et al., 1999
Arabian Sea	Feb'97	-	31±16	-	-	-	-	-	Sarin et al., 1999
Arabian Sea	April-May'94	-	18±6	-	-	-	-	-	Sarin et al., 1999
Arabian Sea	July-Aug'95 July-Aug'96	-	8±3	-	-	-	-	-	Sarin et al., 1999
Arabian Sea	May'95	16±11	20±7	-	-	-	-	-	Johansen et al., 1999
Arabian Sea	July-Aug'95	2.8±1.7	7.4±1.9	-	-	-	-	-	Johansen et al., 1999
Arabian Sea	Mar-April'98	-	19±9	-	-	-	-	-	Rengarajan and Sarin, 2004
Arabian Sea	Dec'07	97±89	50±46	-	-	-	-	-	Kumar et al., 2012
Arabian Sea	Jan-Feb'18	67±9	24±8	-	-	-	-	-	Aswini et al., 2020
Bay of Bengal	Dec'08-Jan'09	171±182	14±10	185±185	59±54	0.73±0.14	0.11±0.16	0.17±0.1	Bikkina et al., 2011
Bay of Bengal	Mar-Apr'06	50+35	1.2+1.4	51+34	17+18	0.68+0.32	0.05+0.09	0.27±0.27	Bikkina et al., 2011
S. China Sea	April'05	-	-	131	65±20	-	-	0.34	(Shi et al., 2010)
Yellow Sea	March'05	-	-	945	204	-	-	0.17	(Shi et al., 2010)
Yellow Sea	April'06	-	-	490	87	-	-	0.17	(Shi et al., 2010)
Qingdao	March'06	-	-	905	199	-	-	0.19	(Shi et al., 2010)
Qingdao	April'06	-	-	458	129	-	-	0.23	(Shi et al., 2010)

E. China Sea	Sep-Oct'02	-	-	-	54 ± 36	-	-	0.24	(Nakamura et al., 2006)
North Pacific	Mar'04	-	-	-	16±19	-	-	0.10	(Nakamura et al., 2006)
Ireland, Mace Head	May'97	-	-	-	130	-	-	0.41	(Spokes et al., 2000)
Ireland, Mace Head	June'96	-	-	-	44	-	-	0.34	(Spokes et al., 2000)
Hawaii (dirty air)	Jan-June'98	-	-	-	29 ± 25	-	-	0.64	(Cornell et al., 2001)
Hawaii (clean air)	Jan-June'98	-	-	-	3 ± 2	-	-	0.31	(Cornell et al., 2001)
Erdemli, Turkey	Mar-May'00	-	-	-	29 ± 42	-	-	0.26±0.28	(Mace et al., 2003b)
Davis, California	Aug'97-Jul'98	-	-	-	19 ± 14	-	-	0.2	(Zhang et al., 2002)

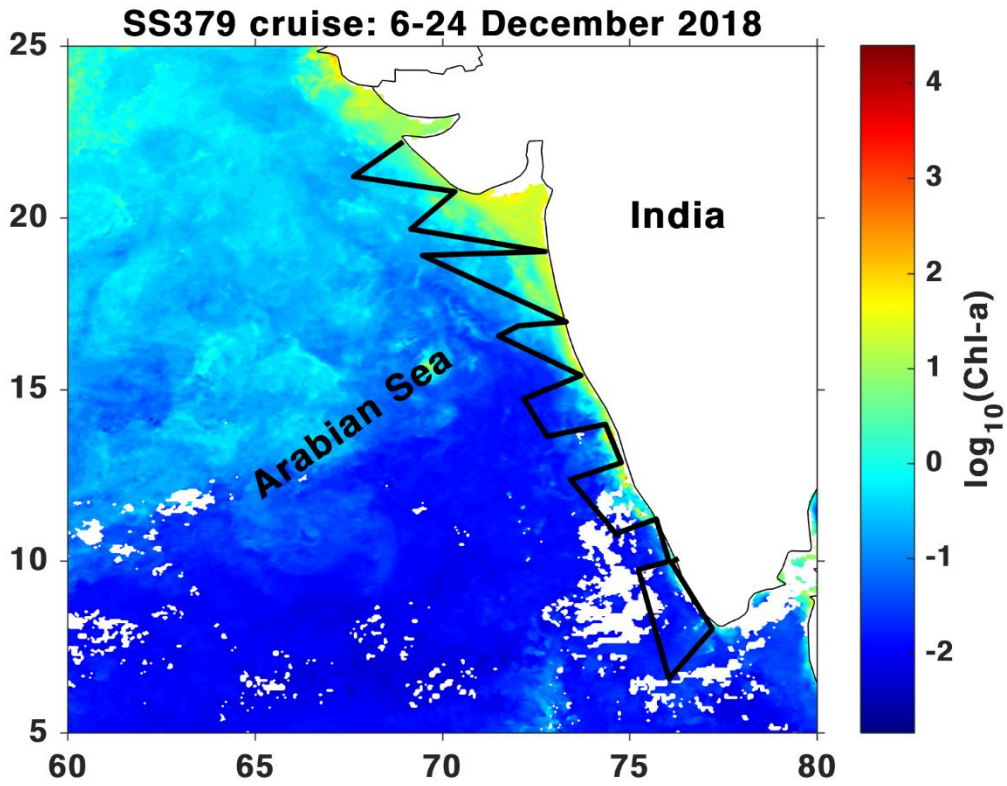

Figure 1. Geographical map depicting the cruise track of SS379 expedition used for aerosol collection along with moderate resolution imaging spectroradiometer (MODIS) satellite-based retrievals of chlorophyll-a concentration (presented in log scale) in the Arabian Sea.

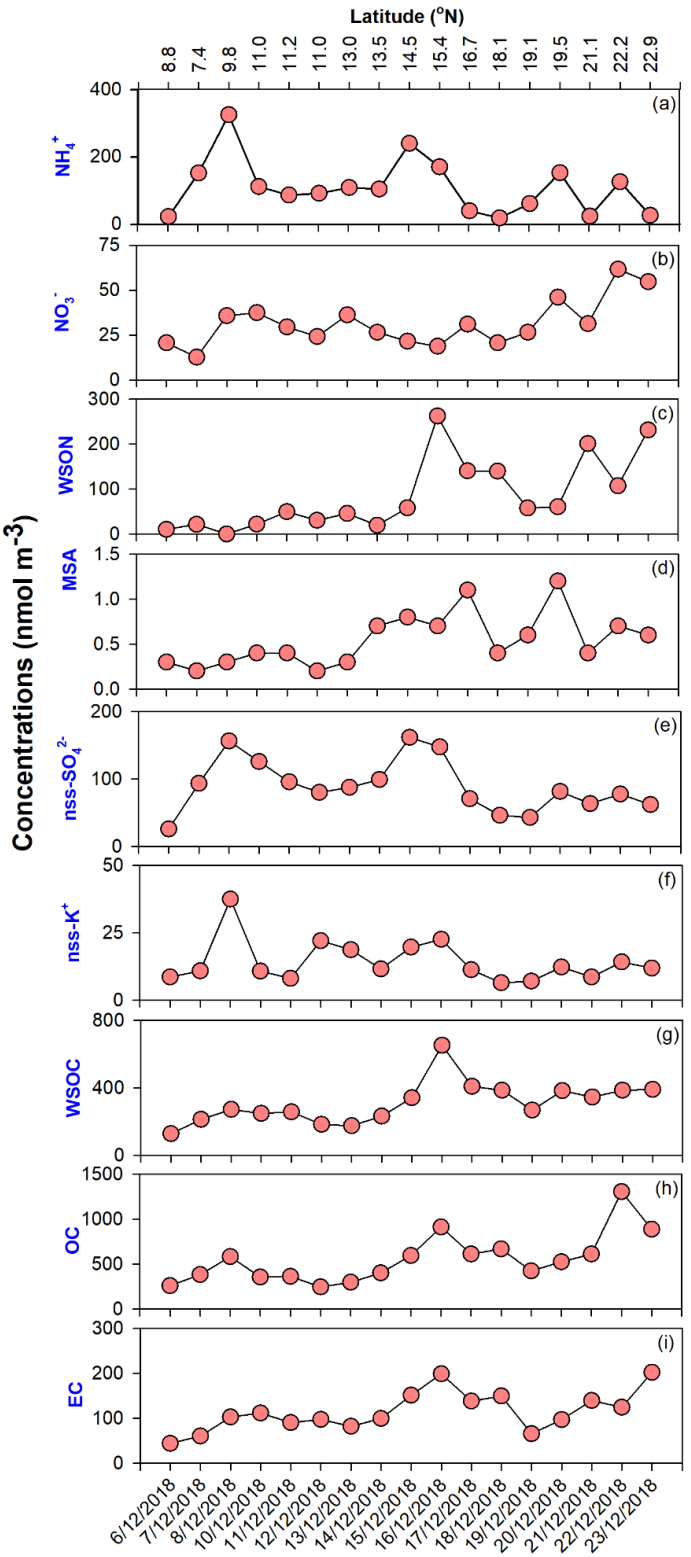

Figure 2. Latitudinal variability of aerosol-N species and other chemical components of TSP samples collected over the Arabian Sea during the SS379 cruise (6-24 December 2018). Here, nss and MSA refer to non-sea-salt component and methanesulfonic acid, respectively.

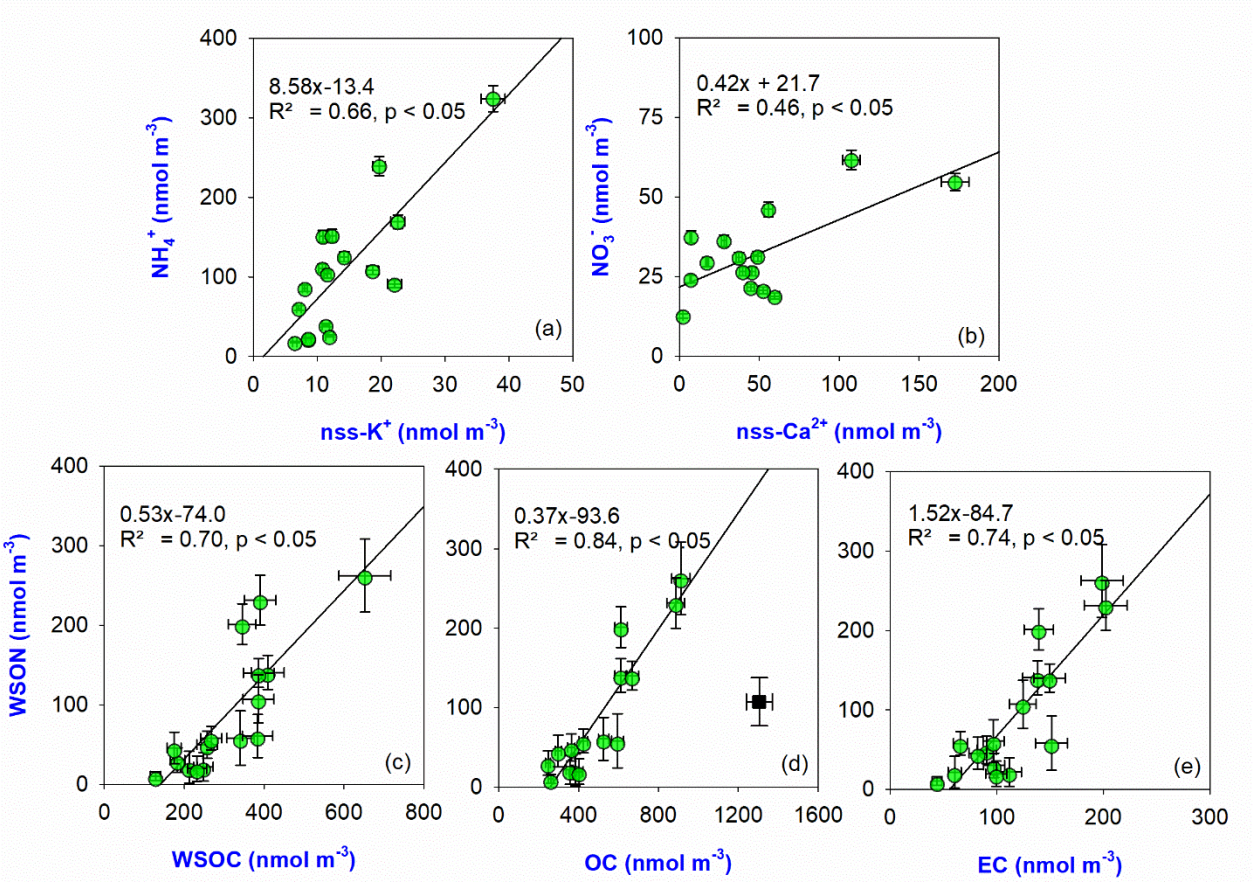

Figure 3. Linear regression analysis between (a) NH_4^+ and WSOC, (b) NO_3^- and nss-Ca^{2+}, between WSON and (c) WSOC (d) OC and (e) EC in the TSP samples collected over the Arabian Sea during SS379 cruise (6-24 December 2018). In panels (a-b) nss-K^+ and nss-Ca^{2+} refer to non-sea-salt component of K^+ (i.e., $[K^+]_{aero}$ - 0.037 × $[Na^+]_{aero}$ and Ca^{2+} ($[Ca^{2+}]_{aero}$ - 0.038 × $[Na^+]_{aero}$), respectively. Here, the factors 0.037 and 0.038 correspond to the weight ratio of K^+ and Ca^{2+} to Na+ in seawater, respectively.

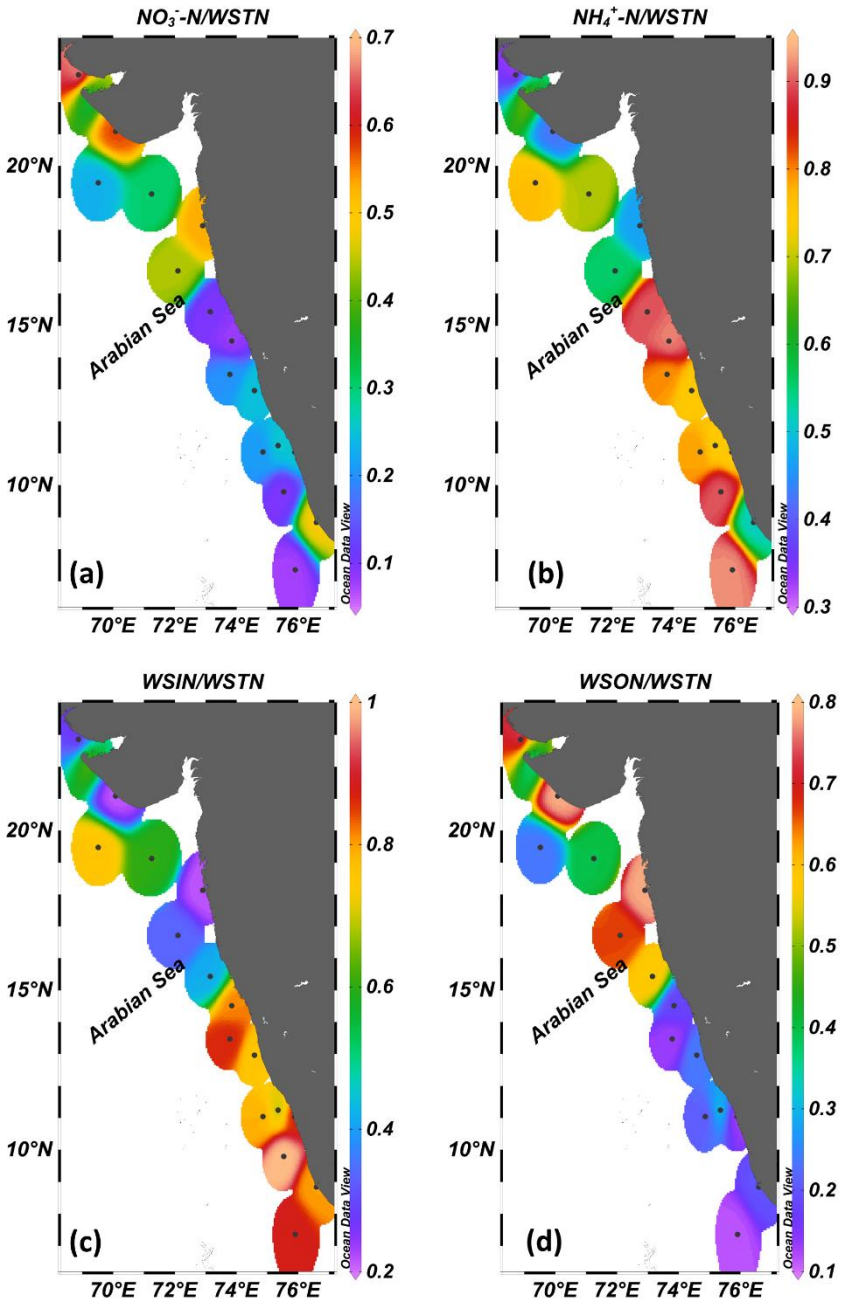

Figure 4. Spatial variability of molar mass ratios of (a) NO_3^-/ WSTN, (b) NH_4^+/WSTN, (c) WSIN/WSTN, (d) WSON/WSTN in the TSP samples collected over the Arabian Sea during SS379 cruise (6-24 December 2018).

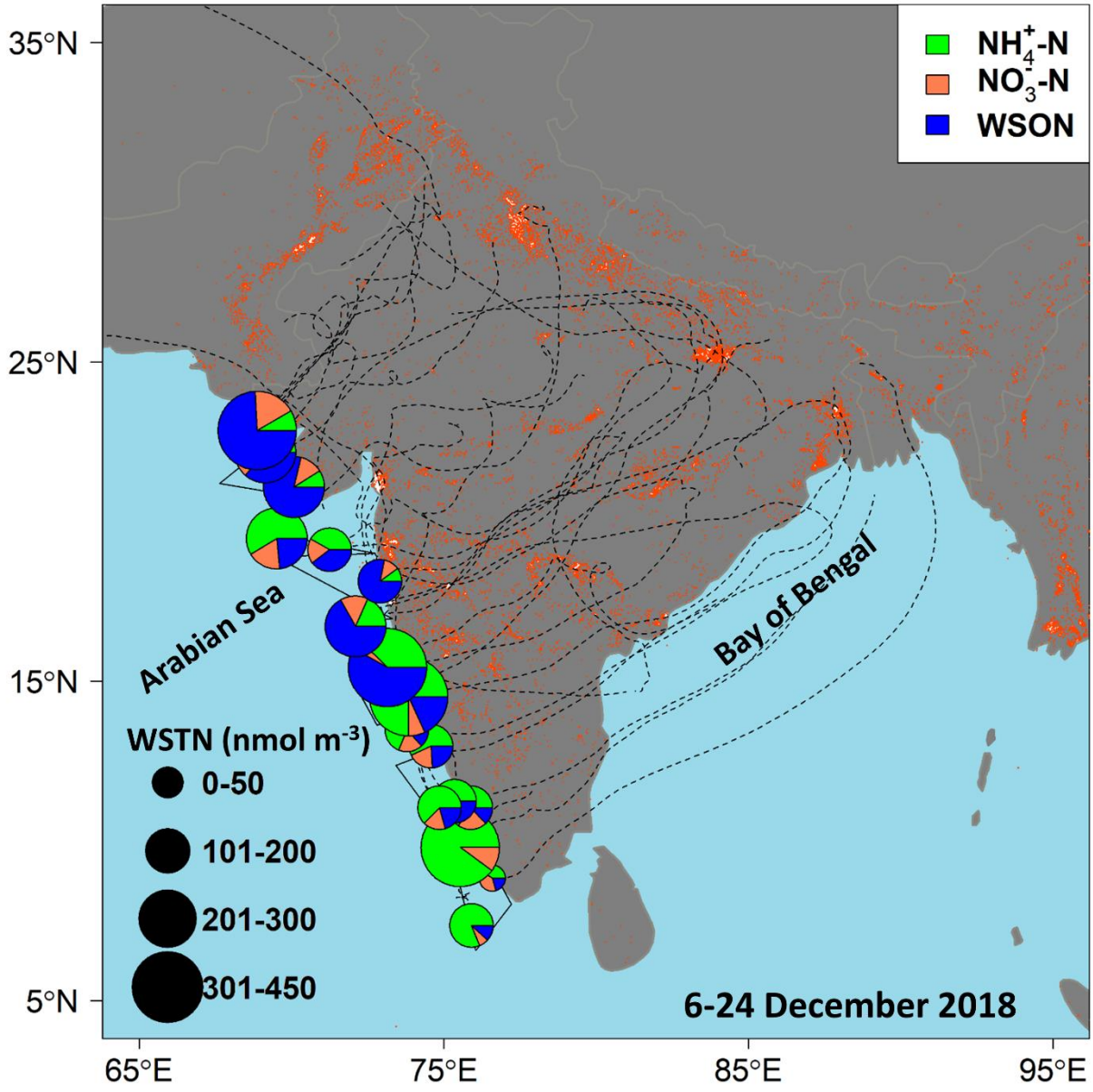

Figure 5. Spatial variability of concentrations of WSTN (size of the circle) along with the constituent percentage contributions of NH_4^+-N, NO_3^- -N, and WSON in marine aerosols collected over the Arabian Sea during the SS379 cruise. Dashed lines represent the 7-day HYSPLIT backward air mass trajectories and red dots are the MODIS fire counts during the cruise.

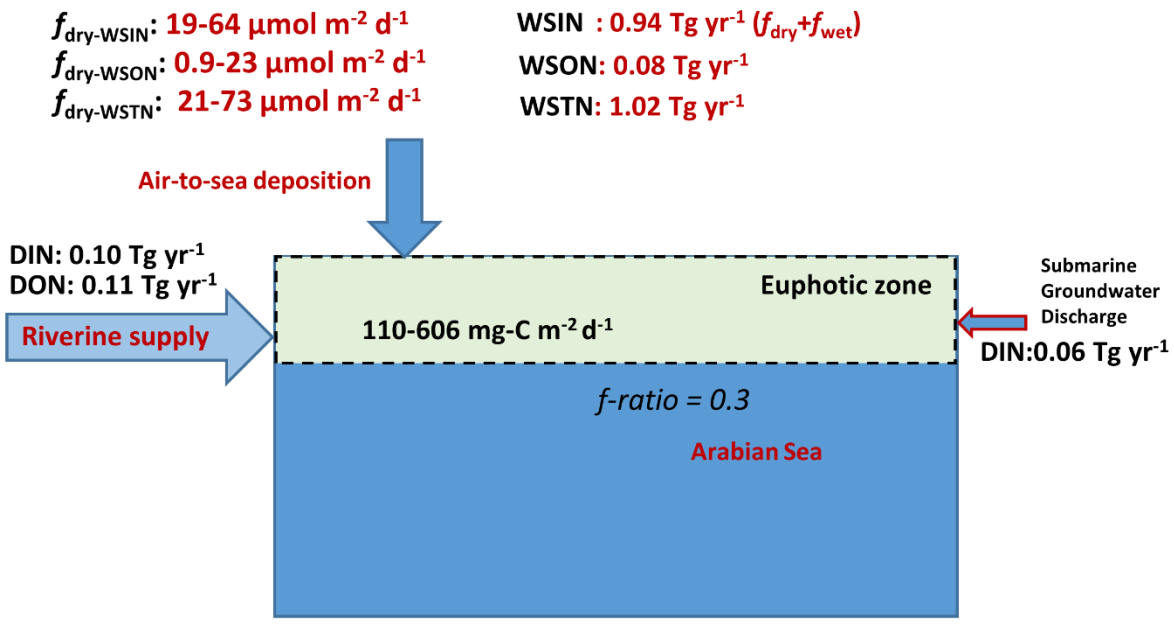

Figure 6. A comparison of the geochemical budget of atmospheric N deposition to the Arabian Sea with the riverine input and in situ water-column primary productivity during the winter season. Here, the f_{wet} refers to the wet deposition flux of WSIN to the Arabian Sea. Also, the DIN and DON corresponds to dissolved inorganic and organic nitrogen data from the riverine supply as well as the DIN input from submarine groundwater discharge (SGD) from the previous publications ((Krishna et al., 2015; Krishna et al., 2016; Kumar et al., 2020)).